

## Fourfold oscillation in anisotropic magnetoresistance and planar Hall effect at the LaAlO<sub>3</sub>/SrTiO<sub>3</sub> heterointerfaces: Effect of carrier confinement and electric field on magnetic interactions

A. Annadi,<sup>1,2</sup> Z. Huang,<sup>1</sup> K. Gopinadhan,<sup>1,3</sup> X. Renshaw Wang,<sup>1,2</sup> A. Srivastava,<sup>1,2</sup> Z. Q. Liu,<sup>1,2</sup> H. Harsan Ma,<sup>1,2</sup> T. P. Sarkar,<sup>1,2</sup> T. Venkatesan,<sup>1,2,3</sup> and Ariando<sup>1,2,\*</sup>

<sup>1</sup>*NUSNNI-Nanocore, National University of Singapore, Singapore 117411, Singapore*

<sup>2</sup>*Department of Physics, National University of Singapore, Singapore 117542, Singapore*

<sup>3</sup>*Department of Electrical and Computer Engineering, National University of Singapore, Singapore 117576, Singapore*

(Received 15 November 2012; revised manuscript received 6 March 2013; published 14 May 2013)

The confinement of the two-dimensional electron gas (2DEG), preferential occupancy of the Ti 3*d* orbital, and strong spin-orbit coupling at the LaAlO<sub>3</sub>/SrTiO<sub>3</sub> interface play a significant role in its emerging properties. Here we report a fourfold oscillation in the anisotropic magnetoresistance (AMR) and planar Hall effect (PHE) at the LaAlO<sub>3</sub>/SrTiO<sub>3</sub> heterointerface. We evaluate the carrier confinement effects on the AMR and find that the fourfold oscillation appears only for the case of 2DEG systems while it is twofold for the three-dimensional system. The AMR behavior is further found to be sensitive to applied electric field, emphasizing the significance of spin-orbit coupling at the interface. These confinement effects suggest that the magnetic interactions are predominant at the interface, and the gate electric field modulation of AMR shows the tunability of magnetic interactions. As the fourfold oscillation fits well to the phenomenological model for a cubic symmetry system, this suggests that the origin of the oscillation may be linked to the anisotropy in magnetic scattering arising from the interaction of electrons with the localized magnetic moments coupled to the crystal symmetry. The observed large PHE further indicates the in-plane nature of magnetic ordering that arises from the in-plane Ti 3*d*<sub>xy</sub> orbitals.

DOI: [10.1103/PhysRevB.87.201102](https://doi.org/10.1103/PhysRevB.87.201102)

PACS number(s): 71.27.+a

### I. INTRODUCTION

The two-dimensional electron gas (2DEG) observed at the LaAlO<sub>3</sub>/SrTiO<sub>3</sub> interface has shown to exhibit multifunctionalities,<sup>1–3</sup> in particular, recently the coexistence of magnetism and superconductivity.<sup>4,5</sup> The existence of magnetic ordering is demonstrated in several ways, such as electronic phase separation,<sup>6</sup> scanning superconducting quantum interference device (SQUID) imaging,<sup>5</sup> torque magnetometry,<sup>7</sup> and magnetotransport measurements<sup>8,9</sup> at low temperatures. At the LaAlO<sub>3</sub>/SrTiO<sub>3</sub> interface, the electrons occupy Ti 3*d* orbitals of the SrTiO<sub>3</sub>. The conductivity arises through the itinerant electrons of Ti 3*d* orbitals, while the origin of magnetic ordering is attributed to the localized Ti 3*d* orbitals. Further, owing to the preferential occupancy, particularly to the Ti 3*d*<sub>xy</sub> orbitals at the interface, various reports have presumed that the magnetization predominantly is in the plane of the interface. The LaAlO<sub>3</sub>/SrTiO<sub>3</sub> interface is also shown to exhibit strong spin-orbit interaction<sup>10,11</sup> due to the broken symmetry near the interface. In this scenario, the confinement of the electron gas at the interface is also expected to influence its orbital occupancy and spin-orbit interaction, and thus its magnetic property. However, the interplay between these magnetic phenomena and the carrier confinement is less understood. A natural way to further probe this is by investigating the in-plane magnetoresistance, i.e., anisotropic magnetoresistance (AMR) and the planar Hall effect (PHE), which directly relate to the magnetic scattering of itinerant electrons associated with the spin-orbit interaction. In this Rapid Communication, we present a comprehensive study of AMR and PHE on the LaAlO<sub>3</sub>/SrTiO<sub>3</sub> based heterointerfaces with respect to the confinement of the electron gas. We find that a fourfold oscillation in AMR is observed only for confined 2DEGs, while a twofold oscillation is observed for the three-dimensional (3D) case. Furthermore, the AMR oscillation is found to depend on the electric field, the magnitude

of the applied magnetic field, and temperature. The obtained results are interpreted in terms of the magnetic ordering and spin-orbit interaction coupled to the symmetry of the system.

### II. METHODS

The LaAlO<sub>3</sub>/SrTiO<sub>3</sub> samples with a LaAlO<sub>3</sub> thickness of 8 unit cells (uc) on TiO<sub>2</sub> terminated SrTiO<sub>3</sub> (001) substrates were grown by pulsed laser deposition (PLD) with *in situ* reflection high energy electron diffraction (RHEED). For the investigation of carrier confinement effects, various samples were grown in different oxygen (O<sub>2</sub>) partial pressures ranging from  $1 \times 10^{-5}$  to  $1 \times 10^{-3}$  Torr. It has been shown that the O<sub>2</sub> pressure during the sample growth can be used to control the dimensionality of the electron gas.<sup>8,12,13</sup> For high O<sub>2</sub> pressure ( $> 1 \times 10^{-4}$  Torr) grown samples, the carrier density  $n_s$  is found to be typically of the order of  $\sim 10^{13}$ – $10^{14}$  cm<sup>-2</sup> with a 2D confined conducting channel, whereas for samples grown at low O<sub>2</sub> pressures ( $\leq 1 \times 10^{-5}$  Torr), the  $n_s$  is of the order of  $10^{16}$  cm<sup>-2</sup> and has a 3D-like conducting channel. Further, we also fabricated LaAlO<sub>3</sub>/SrTiO<sub>3</sub> heterointerfaces on an NdGaO<sub>3</sub> (110) substrate, a technique employed recently to grow precise 2DEG.<sup>14,15</sup> In the later configuration the dimensionality of electron gas can be controlled by the thickness of SrTiO<sub>3</sub>. All electrical transport characterizations were carried out by a physical property measurement system (PPMS) assisted with a rotator which enables to perform angle dependence measurements. The AMR and PHE measurements were performed under various parameters including magnetic field and temperature. Further, in-plane MR, gate voltage, and current dependence of AMR were also performed in order to clarify the misalignment and magnetic field wobbling issues in these types of measurements.<sup>16</sup> The carrier density ( $n_s$ )

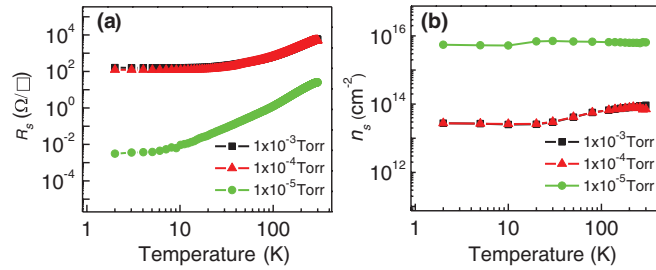


FIG. 1. (Color online) (a) Temperature dependence of sheet resistance  $R_s$  of the  $LaAlO_3/SrTiO_3$  samples grown at various pressures. (b) Carrier density  $n_s$  variation with temperature for corresponding samples.

for the various samples is extracted from conventional Hall measurements.

### III. AMR AND PHE MEASUREMENTS

Figure 1(a) shows the temperature dependence of the sheet resistance  $R_s(T)$  for the samples grown at various  $O_2$  pressures. The high pressure samples show a typical metallic behavior with higher  $R_s$  when compared to the one grown at low  $O_2$  pressure. The  $O_2$  pressure dependence of  $R_s(T)$  shown here is consistent with earlier reports.<sup>8,13</sup> Figure 1(b) shows the  $n_s$  dependence with temperature for the corresponding

samples. For the high  $O_2$  pressure samples, the  $n_s$  is of the order of  $6 \times 10^{13} \text{ cm}^{-2}$  at 300 K and  $2.5 \times 10^{13} \text{ cm}^{-2}$  at 2 K, whereas for the low pressure sample the  $n_s$  is about  $8 \times 10^{15} \text{ cm}^{-2}$  at 300 K and  $7 \times 10^{15} \text{ cm}^{-2}$  at 2 K. The origin of large  $n_s$  in low  $O_2$  pressure samples is due to the creation of oxygen vacancies in  $SrTiO_3$ . The dimensionality of electron gas based on  $n_s$  has been previously investigated through various experiments.<sup>12,17</sup>

We first investigate the AMR effect on the  $LaAlO_3/SrTiO_3$  samples grown at high  $O_2$  pressure, i.e., on the confined 2DEG. In the AMR measurement, both the magnetic field ( $\mathbf{H}$ ) and current ( $\mathbf{I}$ ) are in the plane of the sample, and the angle between  $\mathbf{H}$  and  $\mathbf{I}$  is varied from  $0^\circ$  to  $360^\circ$ . Here,  $\mathbf{I}$  is fixed along the  $\langle 100 \rangle$  direction (depicted in Fig. 2). Figure 2(a) shows the AMR measured at 2 K with varying  $\mathbf{H}$  from 3 to 9 T on the sample grown at  $1 \times 10^{-4}$  Torr, where the AMR is defined as  $AMR = [R(\theta) - R(0)] / R(0) \times 100\%$ , where  $\theta$  is the angle between  $\mathbf{H}$  and  $\mathbf{I}$ , and  $R(0)$  is the resistance when  $\mathbf{H}$  and  $\mathbf{I}$  are parallel to each other. For the AMR measured at 9 T, a clear fourfold oscillation appears in the AMR with resistance minima appearing at an angle  $45^\circ$  to the principal  $\{100\}$  directions with a repetition interval of  $90^\circ$ . Further, when  $\mathbf{H}$  is decreased, a clear decrease in the amplitude of the fourfold oscillation and simultaneously a gradual transformation from fourfold to twofold (with two resistance maxima now) oscillation are observed. At  $\mathbf{H} = 3$  T the oscillations turn completely into twofold with resistance

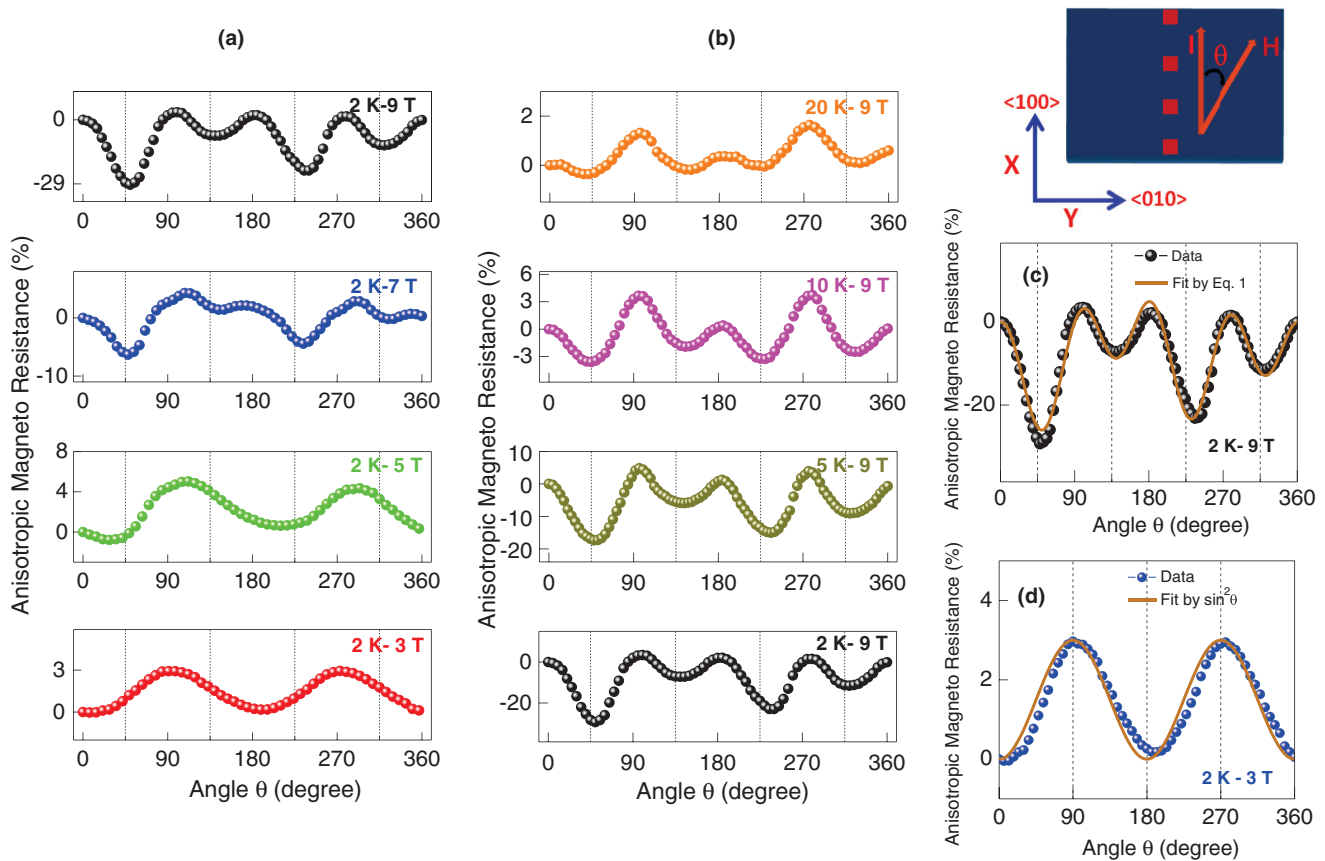


FIG. 2. (Color online) AMR measured for the  $LaAlO_3/SrTiO_3$  interface prepared at  $1 \times 10^{-4}$  Torr for, (a) different magnetic fields at 2 K, and (b) different temperatures at 9 T. (c) A phenomenological model formula fit to the AMR obtained at 2 K and 9 T. (d)  $\sin^2 \theta$  fit for the AMR at 2 K and 3 T.

maxima appearing at  $90^\circ$  and  $270^\circ$  with an interval of  $180^\circ$ . A noticeable observation here is the change of the AMR sign from negative for the fourfold oscillation to positive for the twofold oscillation. Figure 2(b) shows the AMR measured with varying temperature from 2 to 20 K at  $H = 9$  T. The fourfold response in the AMR gradually decreases when temperature increases and simultaneously a twofold component emerges. The fourfold oscillation behavior in AMR has been previously reported in magnetic systems such as manganites<sup>18–21</sup> and  $\text{Fe}_3\text{O}_4$ .<sup>22</sup> Very recently, a similar kind of signature of AMR is also observed at the  $\text{LaAlO}_3/\text{SrTiO}_3$  interface.<sup>23–25</sup> Strikingly, all the above mentioned systems possess a  $d$ -orbital character. This suggests that the magnetic interactions arising from the  $d$  orbitals is crucial for the observed fourfold oscillation.

A phenomenological model is widely used to quantitatively describe the AMR and PHE in various  $3d$  ferromagnetic systems.<sup>26–28</sup> In this model, the resistivity tensor is expressed in terms of the direction of current with respect to the applied magnetic field. The fourfold oscillation behavior in the AMR is suggested to be arising from the contribution of higher order terms in the resistivity tensor relating to the crystal symmetry of the system.<sup>26</sup> For the cubic symmetry system, the variation in resistance with angle ( $\theta$ ) is expected to follow the equation containing the direction cosines of higher order, given by

$$R_{XX} = C_0 + C_1 \cos^2(\theta + \theta_c) + C_2 \cos^4(\theta + \theta_c), \quad (1)$$

$$R_{XY} = C_3 \sin 2\theta. \quad (2)$$

Here  $R_{XX}$  corresponds to the AMR whereas  $R_{XY}$  corresponds to the PHE. The coefficients  $C_1$ ,  $C_2$ , and  $C_3$  are considered to arise from the uniaxial and cubic components of magnetization, and  $C_0$  and  $\theta_c$  are additive constants introduced to take the observed asymmetry in the magnitude in the four oscillations into account. Figure 2(c) shows the fitting for the experimental data by Eq. (1), showing a good agreement with the above formula. The further striking observation is the asymmetry in magnitude among four oscillations. If one considers just the crystalline anisotropy, then symmetry is expected in these fourfold oscillations. The fact that we see an asymmetry strongly suggests that there is a further uniaxial anisotropy present in the system. Such anisotropy with respect to the crystal symmetry probably arises because of Fermi surface reconstruction of the various  $3d$  orbitals at the interface. The good agreement of experimental data with the model implies the predominant role of crystal symmetry on the magnetic interactions at the  $\text{LaAlO}_3/\text{SrTiO}_3$  interface.

Further, the twofold oscillation observed at 2 K and 3 T is found to follow a  $\sin^2 \theta$  dependency. The corresponding  $\sin^2 \theta$  fit for the twofold oscillation is shown in Fig. 2(d), which matches the experimental data accurately. The origin of the twofold oscillation can be from the Lorentz scattering of charge carriers, which follows the  $\sin^2 \theta$  dependency. The transformation of the fourfold to twofold oscillations infers that there are two competing components (spin and charge scatterings) for the AMR, and their contribution to AMR depends on parameters such as magnetic field and temperature.

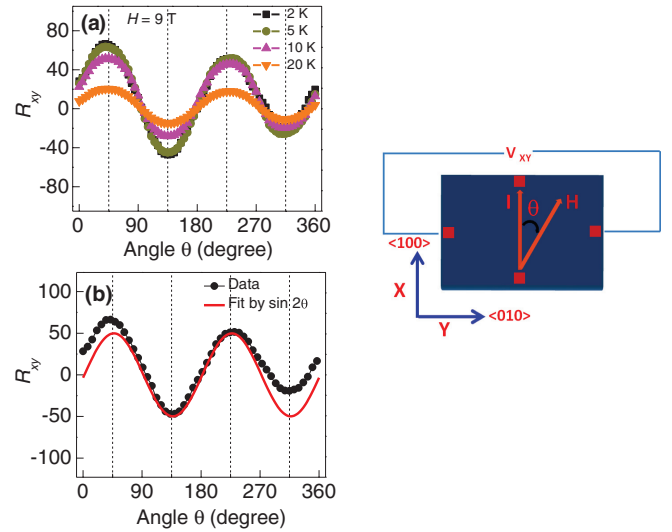


FIG. 3. (Color online) (a) PHE measured for the  $\text{LaAlO}_3/\text{SrTiO}_3$  interface prepared at  $1 \times 10^{-4}$  Torr at various temperatures. (b)  $\sin 2\theta$  fit for the PHE obtained at 2 K and 9 T.

The evolution of fourfold oscillation from twofold oscillation for the magnetic field  $H > 3$  T implies that a critical field strength is needed for the coherent magnetic scattering to overcome the charge scattering. Furthermore, the signature of the AMR starts to diminish for higher temperatures (above 20 K), which could be due to the diminishing of coherence scattering as thermal fluctuations emerge strongly.

To further study the anisotropy we performed PHE measurement. The PHE is similar to the AMR which arises from magnetic related anisotropy. In PHE measurements,  $I$  and  $H$  are in the plane of the sample and the angle between  $H$  and  $I$  is varied between  $0^\circ$  and  $360^\circ$ . Unlike AMR, here the resistivity is measured using Hall geometry, i.e., transverse resistance  $R_{XY}$  (depicted in Fig. 3). Figure 3(a) shows the  $R_{XY}$  measured at  $H = 9$  T with respect to angle ( $\theta$ ) by varying the temperature. The maxima (which are positive) and minima (which are negative) in  $R_{XY}$  appear at  $45^\circ$  to the principal  $\{010\}$  directions with a  $90^\circ$  interval. In general, the PHE contribution to  $R_{XY}$  is expected to follow  $\sin 2\theta$  behavior.<sup>28,29</sup> Figure 3(b) shows a fit to  $\sin 2\theta$  for the PHE measured at 2 K and 9 T, which is in good agreement with the formula. The sign change of the Hall signal with angle is a characteristic of the PHE. Considering the cubic symmetry of the system,<sup>26,27</sup> the AMR can be fourfold and/or twofold, but the PHE is only twofold, which is in fact what we observed in our AHE and PHE (Figs. 2 and 3, respectively). The large planar Hall signal observed here infers a predominant in-plane component for the magnetic ordering at this interface.

From the results presented above it is shown that the samples having confined 2DEGs exhibit strong anisotropy with the evolution of fourfold oscillations in AMR (a similar oscillation behavior in AMR is also observed for the  $\text{LaAlO}_3/\text{SrTiO}_3$  sample grown at  $1 \times 10^{-3}$  Torr, shown in the Supplemental Material).<sup>16</sup> It is noted here that in this  $\text{O}_2$  pressure growth regime (where we observed the fourfold oscillation in AMR) various reports have demonstrated the magnetism at this interface using different techniques, although the strength of

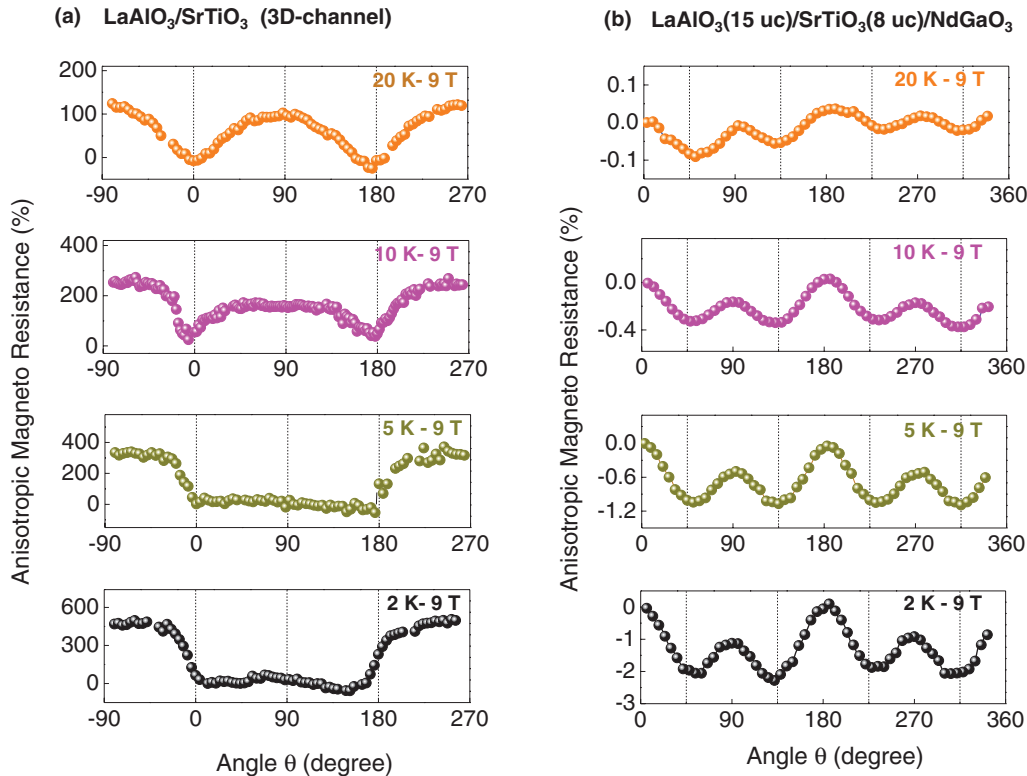


FIG. 4. (Color online) (a) AMR measured for the  $\text{LaAlO}_3/\text{SrTiO}_3$  interface prepared at  $1 \times 10^{-5}$  Torr (3D conducting channel) for different temperatures at 9 T. (b) AMR measured for the  $\text{LaAlO}_3(15 \text{ uc})/\text{SrTiO}_3(8 \text{ uc})/\text{NdGaO}_3$  (110) heterostructure (2D conducting channel) for different temperatures at 9 T.

the magnetic interaction can be further dependent on several sample growth parameters.

#### IV. CARRIER CONFINEMENT EFFECT AND ELECTRIC FIELD EFFECT

To investigate the effect of confinement of the electron gas, we performed AMR measurements on the  $\text{LaAlO}_3/\text{SrTiO}_3$  sample grown at low pressure ( $1 \times 10^{-5}$  Torr) which has a 3D-like conducting channel. Figure 4(a) shows the AMR measured at 9 T with varying temperatures for the corresponding sample. Remarkably, in contrast to high pressure samples, it shows only twofold oscillation throughout the temperature range of 2–20 K. However, an antisymmetric behavior in AMR is noticed between  $0^\circ$ – $180^\circ$  and  $180^\circ$ – $360^\circ$  regimes for the  $\mathbf{I}$  direction with respect to  $\mathbf{H}$  at low temperatures, and it gradually decreases with increasing temperature, suggesting an intrinsic origin for this antisymmetry. We attribute this antisymmetry to the difference in interboundary scattering between the two sides of the conducting channel in the 3D case, i.e., the scattering is stronger at the interface between the  $\text{LaAlO}_3$  and  $\text{SrTiO}_3$  whereas it is weaker inside the  $\text{SrTiO}_3$ . While the electrons scattered toward the interface encounter the sharp boundary to the  $\text{LaAlO}_3$  overlayer, those scattered into the  $\text{SrTiO}_3$  side will see a relatively graded boundary due to the 3D nature of the conducting channel. The decrease in antisymmetry with an increase in temperature can be understood as at elevated temperatures the radius of

the orbital path becomes smaller than the 3D channel width, and thus the electron path is governed by Lorentz scattering, as can be seen from the data that at 20 K the AMR follows  $\sin^2 \theta$  behavior. A similar twofold oscillation behavior was also reported in the AMR of the Ar-irradiated  $\text{SrTiO}_3$ ,<sup>30</sup> which has a 3D conducting channel (with  $n_s \sim 1 \times 10^{17} \text{ cm}^{-2}$ ). To validate the confinement effects, a conducting heterointerface with  $\text{LaAlO}_3(15 \text{ uc})/\text{SrTiO}_3(8 \text{ uc})$  is grown on the  $\text{NdGaO}_3(110)$  substrate.<sup>14,15</sup> In this case the electron gas is precisely confined to 8 uc (i.e., thickness of  $\text{SrTiO}_3$ ). The transport properties of the  $\text{LaAlO}_3(15 \text{ uc})/\text{SrTiO}_3(8 \text{ uc})/\text{NdGaO}_3(110)$  sample is given in the Supplemental Material.<sup>16</sup> Figure 4(b) shows the AMR measured at 9 T with varying temperature (2–20 K) for the corresponding sample. Evidently, here also a fourfold oscillation is observed and further the magnitude of AMR gradually decreases as the temperature is increased. This sample shows a clear fourfold oscillation even up to 20 K, which suggests that these heterostructures might have pronounced magnetic effects. As the conducting channel is confined within the 8 uc, thus strong interface effects are also expected, similar to the high pressure grown  $\text{LaAlO}_3/\text{SrTiO}_3$  interface samples.

Along with carrier confinement effects as shown above, the other most important parameter that can influence AMR is the spin-orbit interaction in the system. At the  $\text{LaAlO}_3/\text{SrTiO}_3$  interfaces, the electric field applied to interface through the back gate voltage has been shown to tune the spin-orbit interaction<sup>10</sup> and also the carrier density,<sup>31</sup> which is further

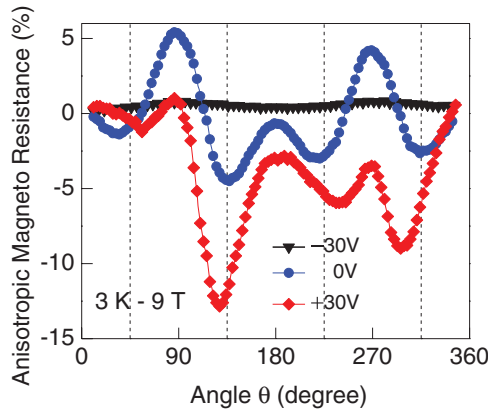


FIG. 5. (Color online) AMR measured for the  $\text{LaAlO}_3/\text{SrTiO}_3$  interface prepared at  $1 \times 10^{-4}$  Torr with various back gate voltages at 3 K and 9 T.

interpreted to influence the preferential  $d$ -orbital filling.<sup>32</sup> To examine the influence of spin-orbit interaction on AMR, we further performed gate electric field dependence of the AMR on the sample grown at  $1 \times 10^{-4}$  Torr. Figure 5 shows the gate voltage dependence of the AMR behavior measured at 3 K and 9 T. The strength of the fourfold oscillation for a +30 V gate voltage is enhanced when compared to the 0 V case. On the other hand, the fourfold oscillation turns into a twofold oscillation for the -30 V gate voltage, showing a strong gate electric field (polarity) dependence of AMR at these interfaces. It suggests that the gate tunable spin-orbit coupling may be the key in the observation of the AMR behavior. The modulation of AMR with electric field effects provides an opportunity to tune the magnetic interactions by the electric field at these interfaces. The electric field modulates the  $n_s$  (in the order of  $\sim 10^{13} \text{ cm}^{-2}$ ) at the interface through the accumulation or depletion of charge, and effectively can also change the  $3d$  orbital fillings and the spin-orbit coupling. Recently, Joshua *et al.*<sup>32</sup> reported that a critical  $n_s$  exists for the  $\text{LaAlO}_3/\text{SrTiO}_3$  interfaces, where it is shown that the properties of interfaces are strongly influenced by the preferential occupancy of  $3d$  orbitals below and above this critical limit. This may be applicable to our samples also; however, the critical  $n_s$  values may depend on the mobility values as suggested. From the above observations, it is evident that the confinement of the electron gas and the spin-orbit interaction strength at the interface are very crucial for the fourfold oscillation in AMR. For the case of confined 2DEG, numerous experimental and theoretical reports illustrated that, near the  $\text{LaAlO}_3/\text{SrTiO}_3$  interface, the Ti  $3d$  orbitals undergo crystal-field-induced splitting which leads to a preferential filling<sup>33-35</sup> of  $3d$  orbitals. It is suggested that the electrons preferentially occupy the  $3d_{xy}$  orbitals in the first few layers of  $\text{SrTiO}_3$  (Refs. 33 and 34) from the interface, which is supported by the spectroscopic experiments.<sup>35</sup> Further, the fraction of occupied  $3d_{xy}$  orbitals ( $\text{Ti}^{3+}$ ) near the interface is expected to have a localized character due to lattice coupling and/or disorder, which gives rise to magnetic ordering. Therefore the interaction of itinerant electrons with the localized in-plane  $3d_{xy}$  orbitals in the presence of an external magnetic field

would be the prime source of the observed coherent magnetic scattering.

## V. DISCUSSION

Recently, Trushin *et al.*<sup>36</sup> discussed the combined effects of spin-orbit coupling and crystal symmetry on the evolution of AMR with respect to the orientation of current and magnetic field by considering the interplay between spin-orbit coupling and polarized magnetic moments. The fact that we observe fourfold oscillations (with uniaxial anisotropy), the influence of spin-orbit coupling through the gate electric field, and the magnetic field dependence of AMR suggest that the above scenario could be the governing mechanism for the AMR behaviour at these  $\text{LaAlO}_3/\text{SrTiO}_3$  interfaces. In addition, the fourfold oscillation appears only for the confined 2DEG case, indicating that the magnetic ordering is predominant near the interface. On the other hand for the 3D case, the  $n_s$  is of the order of  $10^{16} \text{ cm}^{-2}$ , and the spatial extension of carriers is deeper from the interface into the  $\text{SrTiO}_3$  side. The consequences of a 3D-like conducting channel are as follows: The interface crystal field would be potentially screened by this large  $n_s$  due to the strong Coulomb interactions. As a result the  $3d$  orbitals would become degenerate in  $\text{SrTiO}_3$  and the strength of the spin-orbit interaction is weakened. Moreover, the large  $n_s$  may result in a reduced magnetic ordering near the interface as the charge localization and interface effects would be minimum. Thus we conclude that the absence of the fourfold oscillation in 3D case is due to a weaker magnetic interaction.

## VI. SUMMARY

In summary, we have shown the AMR and PHE in the  $\text{LaAlO}_3/\text{SrTiO}_3$  system. A fourfold oscillation behavior in the AMR is observed for the confined 2DEG, and a twofold oscillation is observed for the 3D case. The observation of this fourfold behavior only for the confined 2DEG case infers that the magnetic interactions are predominant at the interface. The modulation of AMR with gate electric field effects further provides an opportunity for tuning magnetic interactions via tuning the spin-orbit coupling. The observed PHE suggests that the predominant component of the magnetization is in the plane of the samples. The origin of the fourfold oscillation is attributed to the magnetic interaction of itinerant electrons with localized magnetic moments coupled to crystal symmetry through spin-orbit interaction. The AMR and PHE measurements would be very useful as a probe for magnetic interactions in low dimensional systems.

## ACKNOWLEDGMENT

We thank the National Research Foundation (NRF) Singapore under the Competitive Research Program (CRP) ‘‘Tailoring Oxide Electronics by Atomic Control’’ NRF2008NRF-CRP002-024, National University of Singapore (NUS) cross-faculty grant, and FRC (ARF Grant No. R-144-000-278-112) for financial support.

\*ariando@nus.edu.sg

- <sup>1</sup>A. Ohtomo and H. Y. Hwang, *Nature (London)* **427**, 423 (2004).
- <sup>2</sup>N. Reyren, S. Thiel, A. D. Caviglia, L. Fitting Kourkoutis, G. Hammerl, C. Richter, C. W. Schneider, T. Kopp, A.-S. Ruetschi, D. Jaccard, M. Gabay, D. A. Muller, J.-M. Triscone, and J. Mannhart, *Science* **317**, 1196 (2007).
- <sup>3</sup>S. Thiel, G. Hammerl, A. Schmehl, C. W. Schneider, and J. Mannhart, *Science* **313**, 1942 (2006).
- <sup>4</sup>M. M. Mehta, D. A. Dikin, C. W. Bark, S. Ryu, C. M. Folkman, C. B. Eom, and V. Chandrasekhar, *Nat. Commun.* **3**, 955 (2012).
- <sup>5</sup>Julie A. Bert, B. Kalisky, C. Bell, M. Kim, Y. Hikita, and H. Y. Hwang, *Nat. Phys.* **7**, 767 (2011).
- <sup>6</sup>Ariando, X. Wang, G. Baskaran, Z. Q. Liu, J. Huijben, J. B. Yi, A. Annadi, A. Roy Barman, A. Rusydi, Y. P. Feng, J. Ding, H. Hilgenkamp, and T. Venkatesan, *Nat. Commun.* **2**, 188 (2011).
- <sup>7</sup>Lu Li, C. Richter, J. Mannhart, and R. C. Ashoori, *Nat. Phys.* **7**, 762 (2011).
- <sup>8</sup>A. Brinkman, M. Huijben, M. Van Zalk, J. Huijben, U. Zeitler, J. C. Maan, W. G. Van Der Wiel, G. Rijnders, D. H. A. Blank, and H. Hilgenkamp, *Nat. Mater.* **6**, 493 (2007).
- <sup>9</sup>D. A. Dikin, M. Mehta, C. W. Bark, C. M. Folkman, C. B. Eom, and V. Chandrasekhar, *Phys. Rev. Lett.* **107**, 056802 (2011).
- <sup>10</sup>A. D. Caviglia, M. Gabay, S. Gariglio, N. Reyren, C. Cancellieri, and J.-M. Triscone, *Phys. Rev. Lett.* **104**, 126803 (2010).
- <sup>11</sup>M. Ben Shalom, M. Sachs, D. Rakhmilevitch, A. Palevski, and Y. Dagan, *Phys. Rev. Lett.* **104**, 126802 (2010).
- <sup>12</sup>M. Basletic, J.-L. Maurice, C. Carrétéro, G. Herranz, O. Copie, M. Bibes, É. Jacquet, K. Bouzehouane, S. Fusil, and A. Barthélémy, *Nat. Mater.* **7**, 621 (2008).
- <sup>13</sup>W. Siemons, G. Koster, H. Yamamoto, W. A. Harrison, G. Lucovsky, T. H. Geballe, D. H. A. Blank, and M. R. Beasley, *Phys. Rev. Lett.* **98**, 196802 (2007).
- <sup>14</sup>C. W. Bark, D. A. Felker, Y. Wang, Y. Zhang, H. W. Jang, C. M. Folkman, J. W. Park, S. H. Baek, H. Zhou, D. D. Fong, X. Q. Pan, E. Y. Tsybmal, M. S. Rzchowski, and C. B. Eom, *Proc. Natl. Acad. Sci. USA* **108**, 4720 (2011).
- <sup>15</sup>Z. Huang, X. Wang, Z. Q. Liu, W. M. Lü, S. W. Zeng, A. Annadi, W. L. Tan, Y. L. Zhao, T. Venkatesan, and Ariando (submitted for publication).
- <sup>16</sup>See Supplemental Material at <http://link.aps.org/supplemental/10.1103/PhysRevB.87.201102> for AMR measurements performed for different samples under various external parameters.
- <sup>17</sup>X. Wang, W. M. Lü, A. Annadi, Z. Q. Liu, K. Gopinadhan, S. Dhar, T. Venkatesan, and Ariando, *Phys. Rev. B* **84**, 075312 (2011).
- <sup>18</sup>A. W. Rushforth, K. Vyborny, C. S. King, K. W. Edmonds, R. P. Campion, C. T. Foxon, J. Wunderlich, A. C. Irvine, P. Vasek, V. Novak, K. Olejnik, J. Sinova, T. Jungwirth, and B. L. Gallagher, *Phys. Rev. Lett.* **99**, 147207 (2007).
- <sup>19</sup>Y. Q. Zhang, H. Meng, X. W. Wang, X. Wang, H. H. Guo, Y. L. Zhu, T. Yang, and Z. D. Zhang, *Appl. Phys. Lett.* **97**, 172502 (2010).
- <sup>20</sup>M. Bibes, V. Laukhin, S. Valencia, B. Martinez, J. Fontcuberta, O. Yu. Gorbenco, A. R. Kaul, and J. L. Martinez, *J. Phys.: Condens. Matter* **17**, 2733 (2005).
- <sup>21</sup>J. D. Fuhr, M. Granada, L. B. Steren, and B. Alascio, *J. Phys.: Condens. Matter* **22**, 146001 (2010).
- <sup>22</sup>R. Ramos, S. K. Arora, and I. V. Shvets, *Phys. Rev. B* **78**, 214402 (2008).
- <sup>23</sup>M. Ben Shalom, C. W. Tai, Y. Lereah, M. Sachs, E. Levy, D. Rakhmilevitch, A. Palevski, and Y. Dagan, *Phys. Rev. B* **80**, 140403(R) (2009).
- <sup>24</sup>E. Flekser, M. Ben Shalom, M. Kim, C. Bell, Y. Hikita, H. Y. Hwang, and Y. Dagan, *Phys. Rev. B* **86**, 121104(R) (2012).
- <sup>25</sup>A. Joshua, J. Ruhman, S. Pecker, E. Altman, and S. Ilani, *arXiv:1207.7220* (2012).
- <sup>26</sup>T. R. McGuire and R. I. Potter, *IEEE Trans. Magn.* **11**, 1018 (1975).
- <sup>27</sup>J. Li, S. L. Li, Z. W. Wu, S. Li, H. F. Chu, J. Wang, Y. Zhang, H. Y. Tian, and D. N. Zheng, *J. Phys: Condens. Matter* **22**, 146006 (2010).
- <sup>28</sup>A. M. Nazmul, H. T. Lin, S. N. Tran, S. Ohya, and M. Tanaka, *Phys. Rev. B* **77**, 155203 (2008).
- <sup>29</sup>S. Nakagawa, I. Sasaki, and M. Naoe, *J. Appl. Phys.* **91**, 8354 (2002).
- <sup>30</sup>F. Y. Bruno, J. Tornos, M. Gutierrez del Olmo, G. Sanchez Santolino, N. M. Nemes, M. Garcia-Hernandez, B. Mendez, J. Piqueras, G. Antorrena, L. Morellón, J. M. De Teresa, M. Clement, E. Iborra, C. Leon, and J. Santamaria, *Phys. Rev. B* **83**, 245120 (2011).
- <sup>31</sup>A. D. Caviglia, S. Gariglio, N. Reyren, D. Jaccard, T. Schneider, M. Gabay, S. Thiel, G. Hammerl, J. Mannhart, and J.-M. Triscone, *Nature (London)* **456**, 624 (2008).
- <sup>32</sup>A. Joshua, S. Pecker, J. Ruhman, E. Altman, and S. Ilani, *Nat. Commun.* **3**, 1129 (2012).
- <sup>33</sup>Z. S. Popović, S. Satpathy, and R. M. Martin, *Phys. Rev. Lett.* **101**, 256801 (2008).
- <sup>34</sup>P. Delugas, A. Filippetti, V. Fiorentini, D. I. Bilc, D. Fontaine, and P. Ghosez, *Phys. Rev. Lett.* **106**, 166807 (2011).
- <sup>35</sup>M. Salluzzo, J. C. Cezar, N. B. Brookes, V. Bisogni, G. M. De Luca, C. Richter, S. Thiel, J. Mannhart, M. Huijben, A. Brinkman, G. Rijnders, and G. Ghiringhelli, *Phys. Rev. Lett.* **102**, 166804 (2009).
- <sup>36</sup>M. Trushin, K. Výborný, P. Moraczewski, A. A. Kovalev, J. Schliemann, and T. Jungwirth, *Phys. Rev. B* **80**, 134405 (2009).